INTERACTION ENERGY ANALYSES OF FOLATE ANALOG BINDING TO HUMAN DIHYDROFOLATE REDUCTASE: CONTRIBUTION OF THE ANTIFOLATE SUBSTRUCTURAL REGIONS TO COMPLEX STABILITY

Conrad Pitts[1,3], Donnell Bowen[2,3] and William M. Southerland[1,3]*

[1]Department of Biochemistry and Molecular Biology, [2]Department of Pharmacology and [3]The Howard University Drug Discovery Unit, Howard University College of Medicine, Washington, D.C. 20059, USA

SUMMARY

The three-dimensional structure of the human dihydrofolate reductase (DHFR), methotrexate tetrazole, and NADPH ternary complex was used to model the corresponding ternary complexes with methotrexate tetrazole replaced by methotrexate, methotrexate-polyglutamate with three glutamyl residues, and 5,10-deazaaminopterin, respectively. Each complex was solvated in a 60-angstrom cube of explicit water and subjected to structural minimization followed by interaction energy analyses. Interaction energy calculations were performed for the antifolate interaction with water, NADPH, the DHFR binding site residues, the entire DHFR protein, and the solvated NADPH:DHFR complex. These studies revealed that methotrexate-polyglutamate exhibited the most stable interactions and that approximately one half of antifolate:DHFR stability could be accounted for by the interaction of the antifolate with the binding site residues. The antifolate structures were also subdivided into hetero-

* Author for correspondence:
Dr. William M. Southerland
Department of Biochemistry and Molecular Biology
Howard University College of Medicine
520 "W" Street NW
Washington, D.C. 20059, USA
e-mail: wsoutherland@howard.edu

cyclic, phenyl, and glutamyl substructural regions. Interaction energies were subsequently calculated for the interactions of the subregions with water, NADPH, the DHFR binding site residues, the DHFR protein, and the solvated NADPH:DHFR complex. The glutamyl substructural region showed the greatest contribution to overall antifolate binding stability due to its interaction with the DHFR protein. The heterocyclic and phenyl substructural regions generally showed much less stable interactions. These results suggest that the primary stabilizing factor of the antifolate interaction is the interaction of glutamyl with the DHFR protein. Additionally, interaction energy analyses were performed for specific groups of atoms within the substructural regions. These studies indicated that the stability of the glutamyl interaction is due to the interaction of glutamyl oxygen atoms with the DHFR protein. In the case of the methotrexate tetrazole complex, the tetrazole nitrogens also contribute significantly to the stability of the glutamyl interaction. The carbon atoms of the heterocyclic and phenyl groups both showed more stable interactions with NADPH than with water, while the nitrogen atoms showed more stable interactions with water than with NADPH. Collectively, these results indicate that the glutamyl region is the most important in antifolate binding stability.

KEY WORDS

binding energies, antifolate substructural regions, complex stability, human dihydrofolate reductase

INTRODUCTION

Methotrexate (MTX) is a potent inhibitor of dihydrofolate reductase (DHFR) /1,2/. It is structurally similar to folic acid. They each contain heterocyclic, phenyl, and glutamyl substructural regions. These regions participate in binding to DHFR and have been the target of antifolate structural modification studies in the design and development of new DHFR inhibitors. The synthesis of antifolate analogs has provided insight into the contributions of the different antifolate substructural regions to antifolate binding.

Antifolate analogs with structural modification of the glutamyl moiety have been most thoroughly investigated. For example, when the glutamyl group of aminopterin was replaced with aminophosphoalkanoic acid side chains /3/, the aminophosphoalkanoic analogs with 2 (-CH_2-) groups in the alkane chain showed maximal inhibition of DHFR and folylpolyglutamate synthetase activity. These derivatives also inhibited the growth of MTX sensitive (L1210) and insensitive (L1210/R81) cancer cells. Gamma-monoamides of aminopterin and MTX showed IC_{50}s for DHFR inhibition that were 1.5 to 5-fold higher than those observed for the corresponding parent compounds /4/. n-Octyl, n-dodecyl, and n-hexadexyl alpha- and gamma-esters of MTX inhibited DHFR in the following order of potency: MTX > MTX gamma-esters > MTX alpha-esters /5/. In the case of both alpha- and gamma-esters, the shorter chain derivatives were generally more efficient DHFR inhibitors. Replacement of the gamma-carboxyl groups of MTX and aminopterin with tetrazole results in analogs that inhibit DHFR activity as effectively as their corresponding parent compounds /6/. Polyglutamated analogs of antifolates are synthesized intracellularly as a result of the administration of the parent compounds /7,8/. Polyglutamyl derivatives of MTX and 10-deaza-aminopterin consisting of a total of one through six glutamyl groups were tested as DHFR inhibitors /9/. The addition of glutamyl groups caused a progressive increase in the ability of MTX to inhibit DHFR. In the case of 10-deazaaminopterin, the addition of one, two, and three glutamyl groups resulted in a decreased ability to inhibit DHFR, while the addition of the fourth and fifth glutamyl groups caused an increase in DHFR inhibition. These observations indicate that the same modification on different parent antifolates can affect DHFR inhibition differently.

Modification of the heterocyclic ring moiety has indicated that this substructural region is also an important factor in antifolate inhibition of DHFR. B-ring deaza analogs of a nonpolyglutamatable DHFR inhibitor (N^{alpha}-(4-amino-4-deoxypteroyl)-N^{delta}-hemiphthaloyl-L-ornithine) showed a variety of DHFR inhibitory effects, depending on the ring location of the deaza function /10/. The 8-deaza, 5,8-deaza, and 5-methyl-5,8-deaza analogs showed Ki values for the inhibition of DHFR that were 1.8, 3.8, and 3.5-fold lower, respectively, than that observed for the unmodified compound /10/. These compounds also effectively inhibited cancer cell growth. The 9-ethyl derivative of 10-

deazaaminopterin and alkyl derivatives of 5-deazaaminopterin and 5-deazamethotrexate behaved similar to the corresponding non-alkylated deaza compounds in their ability to inhibit DHFR /11,12/. These results indicate that replacement of heterocyclic ring nitrogen atoms may be more important to antifolate binding than simply alkylating the existing nitrogen atoms.

Structural changes in the phenyl substructual region have also yielded interesting observations. For example, when analogs of 10-deazaaminopterin and 5-alkyl-5,10-deazaaminopterin were prepared with the phenyl ring replaced by the 4-substituted 1-naphthoyl group, the resulting analogs were more effective than MTX in the inhibition of L1210, S180, and HL60 tumor cell lines /13/.

Studies mentioned above clearly reveal that modification of an antifolate substructural region can effect overall antifolate binding to DHFR and associated therapeutic effects. In fact, the development of new antifolates has relied heavily on the modification of existing antifolate structures. However, the relative contribution of each individual substructural region to overall antifolate binding stability is not well understood. Consequently, it was of interest to calculate the interaction energies for selected antifolates and their heterocyclic, phenyl, and glutamyl substructural regions with the solvated NADPH:human DHFR complex and its components. These studies provide new information on the stability of antifolate binding to DHFR and on the substructural contribution to antifolate binding stability.

MATERIALS AND METHODS

The X-ray determined three-dimensional structure of the methotrexate tetrazole:NADPH:human DHFR was obtained from Dr. Vivian Cody /14/. In separate molecular modeling procedures the methotrexate tetrazole (MTXT) component of this complex was converted to 5,10-deazaaminopterin (DEAZ), methotrexate (MTX), and methotrexate-polyglutamate (MTX-$(glu)_3$), resulting in the following human DHFR complexes: DEAZ:NADPH:DHFR, MTX: NADPH:DHFR, and MTX-$(glu)_3$:NADPH:DHFR. These DHFR complexes in addition to the MTXT:NADPH:DHFR complex were subsequently used to evaluate antifolate:DHFR interaction energies.

Molecular modeling studies were performed using the molecular modeling software Quanta from Biosym Inc. The complexes were modeled inside a 60-angstrom cube of explicit water. The density of water in the cube was approximately 1.0 g/ml. Each complex was subsequently minimized to an energy tolerance gradient of 0.00 kcal/mole/step. Minimizations were performed using the Adopted-Basis Newton Raphson algorithm in CHARMM /15/. After minimization, CHARMM was used to calculate interaction energies. For each complex, the DHFR binding site residues were defined as those DHFR residues which were 4.0 angstroms or closer to the bound antifolate. Energies were calculated for interactions with the solvated NADPH: DHFR complex (complex), the DHFR binding site residues (binding site), the entire DHFR protein only (DHFR), water, and NADPH.

RESULTS

Figure 1 shows the interaction energy analyses of DEAZ, MTX, MTXT, and MTX-$(glu)_3$. Each ligand showed more stable interactions

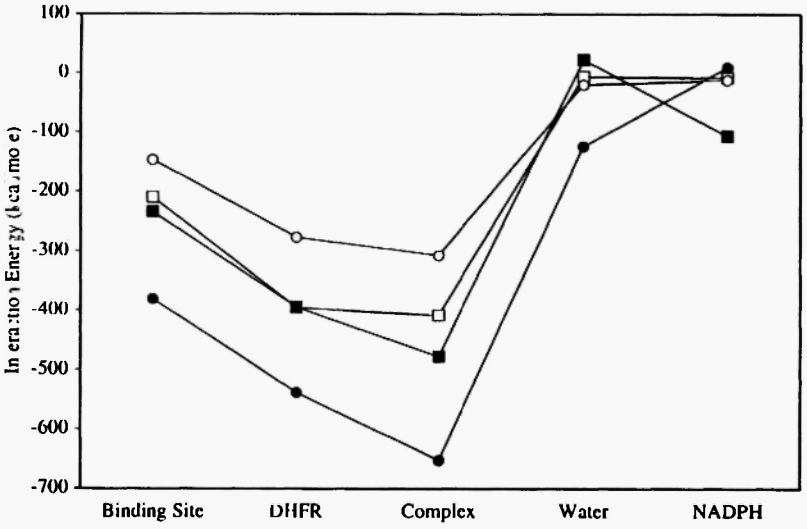

Fig. 1: Interaction energy analysis of 5,10-deazaaminopterin (open squares), MTXT (closed squares), MTX (open circles), and MTX-$(glu)_3$ (closed circles).

with the binding site, DHFR, and complex than with water or NADPH. The antifolate:DHFR interaction energies represent between 82 and 96% of the antifolate:complex interaction energies while the antifolate:binding site interaction energies represent approximately 50% of the antifolate:complex interaction energies (Table 1). These results indicate that the major stabilizing factor of the complexes is the antifolate:DHFR interactions and the antifolate:binding site interactions are the major stabilizing factors of the antifolate:DHFR interactions.

The substructural regions of each antifolate were defined as shown in Figure 2. Figure 3 A-D show the interaction energy analyses for the heterocyclic, phenyl, and glutamyl regions of DEAZ, MTX, MTX-$(glu)_3$, and MTXT, respectively. For each antifolate, the glutamyl group showed significantly more stable energies, particularly with the DHFR and the complex interactions. Additionally, as can be seen in Table 2, the glutamyl:DHFR interaction energies range between 80 and 100% of the glutamyl:complex interaction energies while the glutamyl:binding site interaction energies range between 37 and 55% of the glutamyl:complex interaction energies. Consequently, the glutamyl:DHFR interactions are the primary stabilizing features of the glutamyl:complex interactions and the glutamyl:binding site interactions are significant contributors to the stability of the glutamyl:DHFR interactions. Moreover, Table 3 shows that the glutamyl:DHFR and glutamyl:binding site interactions are the primary contributors to the stability of the overall antifolate:complex interactions. Although the pattern of glutamyl interaction in each complex was similar, the interaction was much more stable in the case of MTXT and MTX-$(glu)_3$, with the latter showing the highest level of stability of all the complexes. These two glutamyl groups are more polar than the glutamyl groups associated with MTX and DEAZ due to the tetrazole ring and the polyglutamate structure, respectively. These observations suggest that increased polarity in the glutamyl substructure is likely an important factor in antifolate interaction energy stability.

The heterocyclic, phenyl, and glutamyl regions of each antifolate were further subdivided into subgroups of carbon, nitrogen, and if applicable oxygen atoms. The interaction energies associated with the heterocyclic subgroups of atoms are shown in Figure 4 A-D. The most striking feature of these results is that the carbon and nitrogen atoms of each heterocyclic ring exhibited opposing and approximately equal

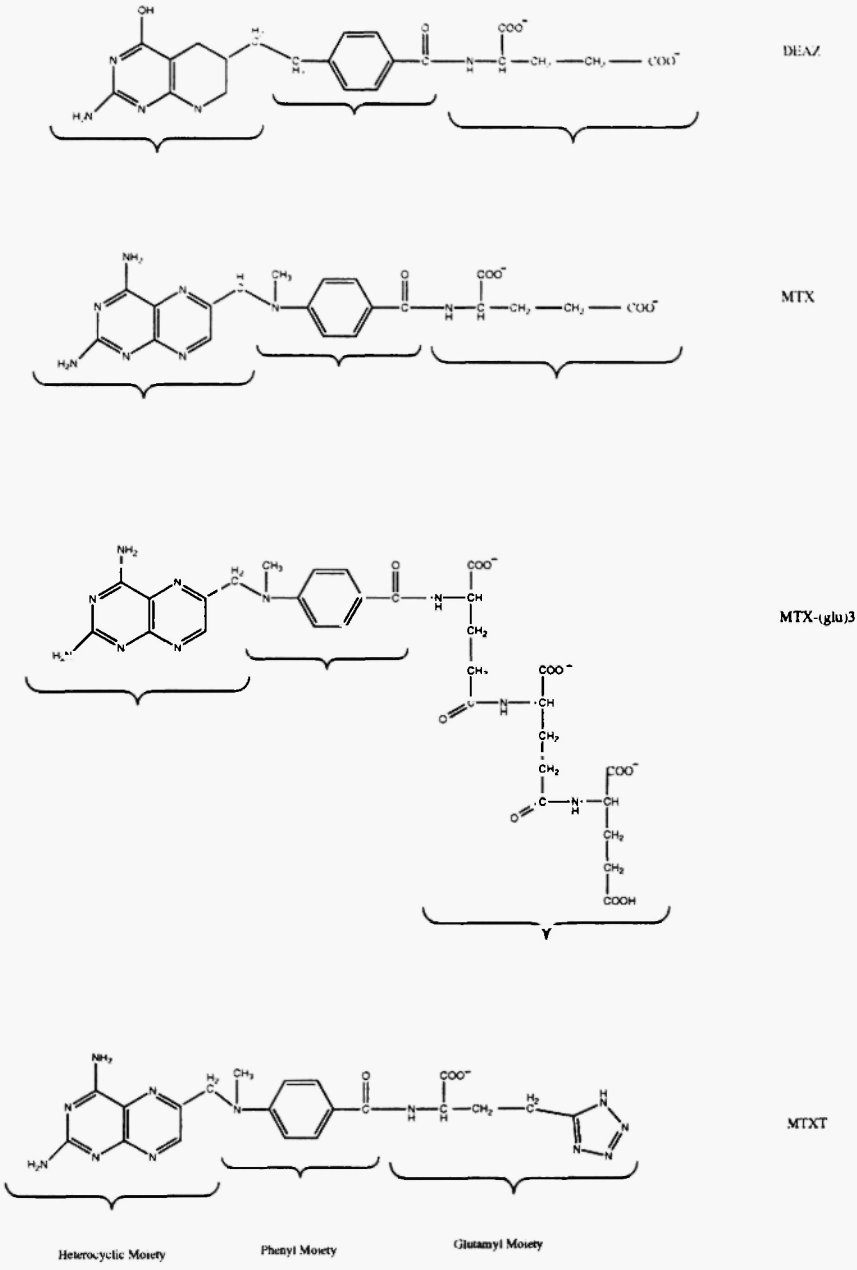

Fig. 2: Subdivision of 5,10-deazaaminopterin, MTXT, MTX, and MTX-$(glu)_3$ into their respective heterocyclic, phenyl, and glutamyl moieties.

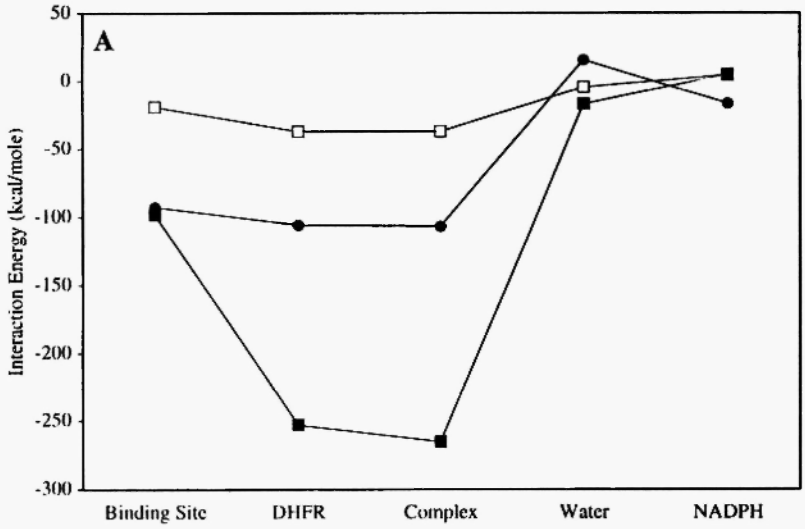

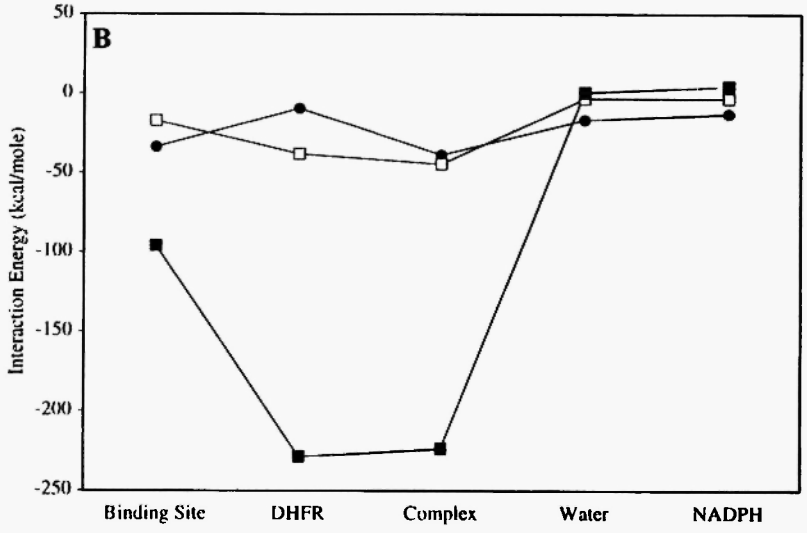

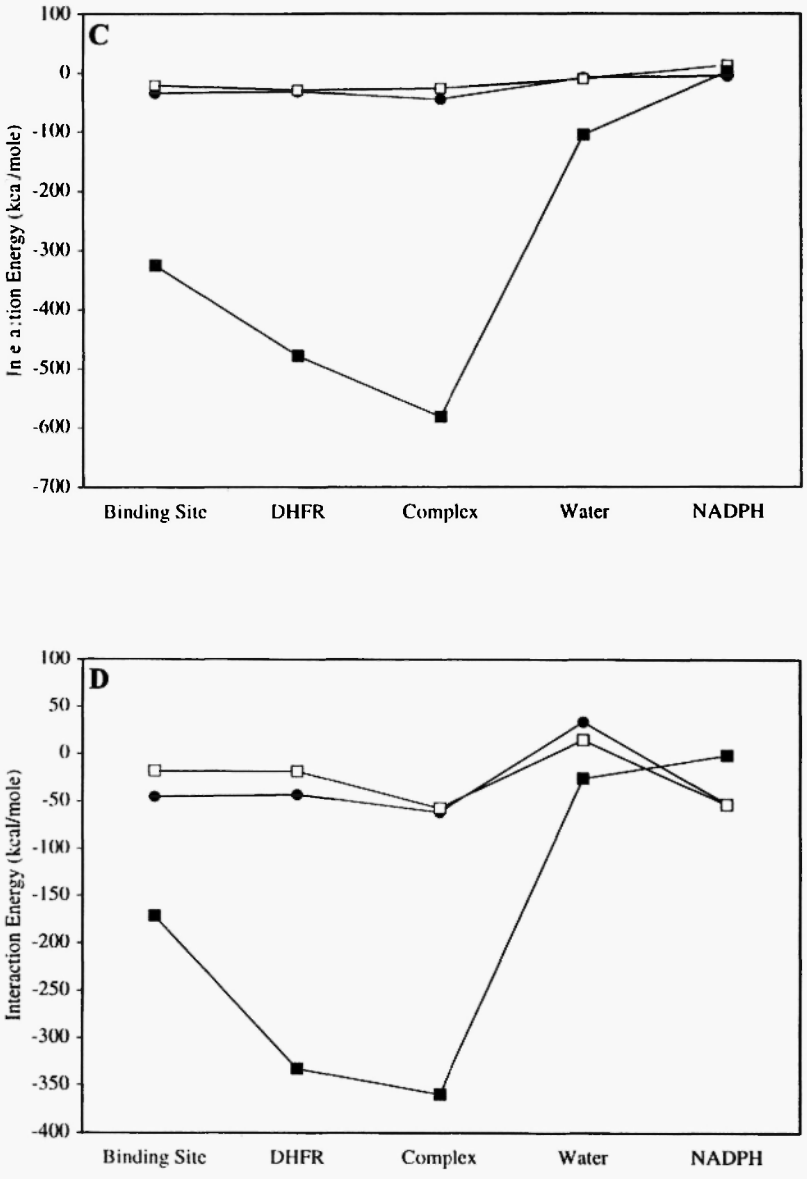

Fig. 3: Interaction energy analysis for the heterocyclic, phenyl, and glutamyl moieties of 5,10-deazaaminopterin (panel A), MTX (panel B), MTX-$(glu)_3$ (panel C), and MTXT (panel D). The heterocyclic, phenyl, and glutamyl moieties are represented by closed circles, open squares, and closed squares, respectively.

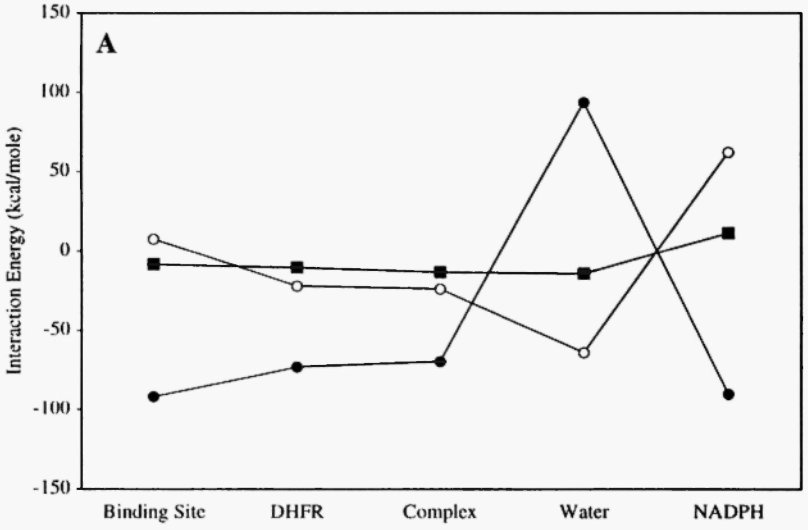

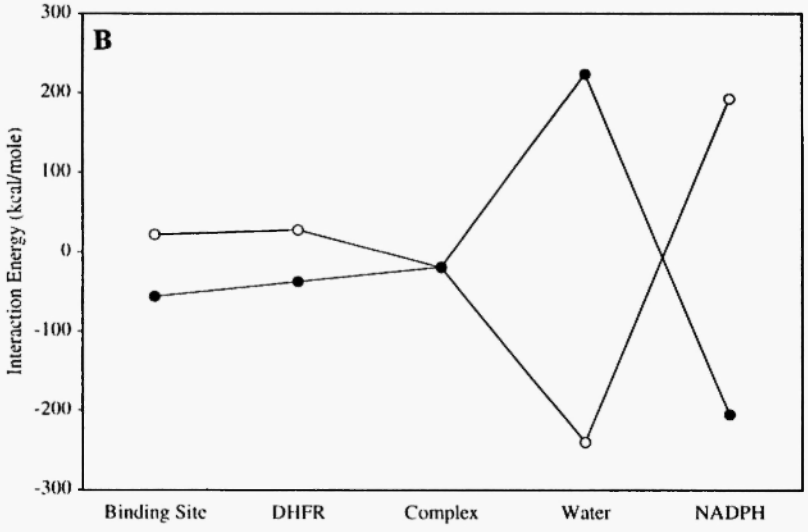

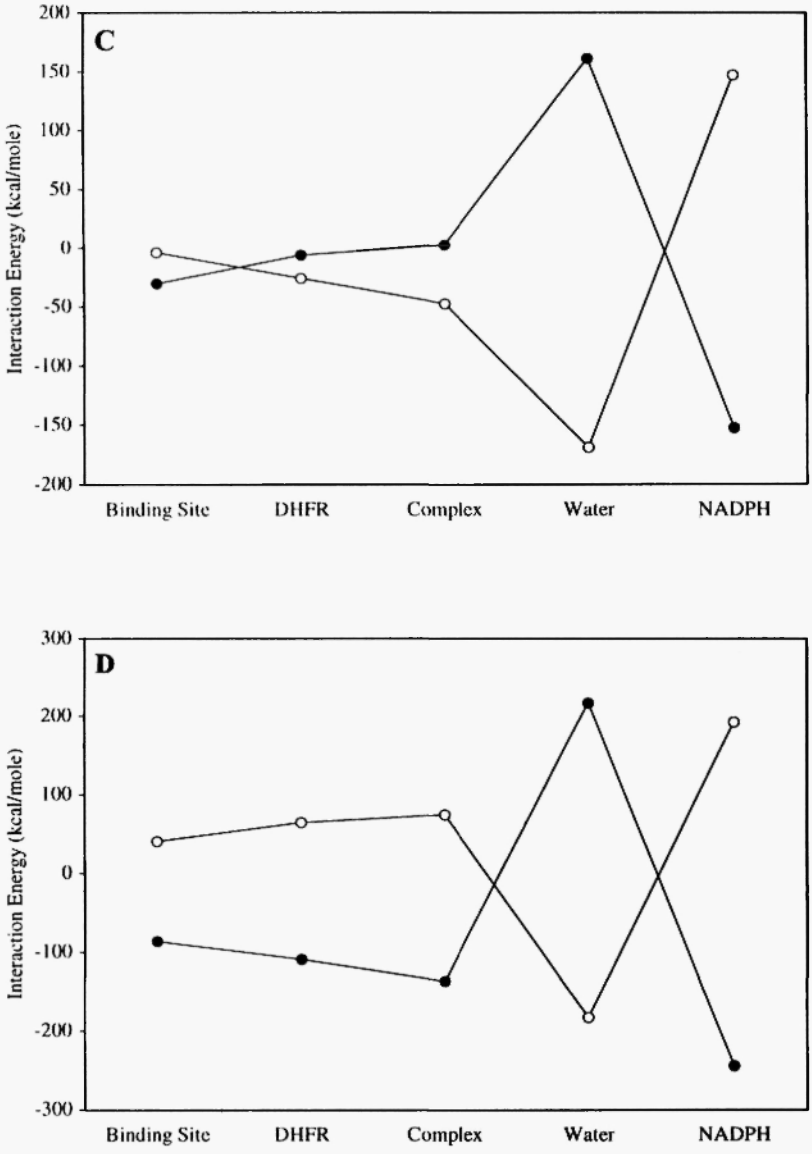

Fig. 4: Interaction energy analysis for the atomic subgroups of the heterocyclic moieties of 5,10-deazaaminopterin (panel A), MTX (panel B), MTX-$(glu)_3$ (panel C) and MTXT (panel D). The nitrogen, carbon, and oxygen atoms are represented by open circles, closed circles, and closed squares, respectively.

TABLE 1

Antifolate:binding site and antifolate:DHFR interaction energies expressed as per cent of the antifolate:complex interaction energy

Antifolate	$\frac{\text{Antifolate:Binding Site}}{\text{Antifolate:Complex}} \times 100$	$\frac{\text{Antifolate:DHFR}}{\text{Antifolate:Complex}} \times 100$
DEAZ	**51.33**	96.77
MTXT	49.01	82.52
MTX	47.85	90.04
MTX-(glu)$_3$	58.36	82.51

TABLE 2

Glutamyl:binding site and glutamyl:DHFR interaction energies expressed as per cent of the glutamyl:complex interaction energy

Antifolate	$\frac{\text{Glutamyl:Binding Site}}{\text{Glutamyl:Complex}} \times 100$	$\frac{\text{Glutamyl:DHFR}}{\text{Glutamyl:Complex}} \times 100$
DEAZ	37.03	95.41
MTXT	47.66	92.51
MTX	42.90	102.31
MTX-(glu)$_3$	55.97	82.12

TABLE 3

Glutamyl:binding site and glutamyl:DHFR interaction energies expressed as per cent of the antifolate:complex interaction energy

Antifolate	$\frac{\text{Glutamyl:Binding Site}}{\text{Antifolate:Complex}} \times 100$	$\frac{\text{Glutamyl:DHFR}}{\text{Antifolate:Complex}} \times 100$
DEAZ	24.03	61.79
MTXT	35.88	69.64
MTX	31.28	74.59
MTX-(glu)$_3$	49.90	73.22

interaction energies with water and NADPH. The carbon atoms showed favorable interactions with NADPH and the nitrogens showed favorable interactions with water. Therefore, the heterocyclic ring may contribute to DHFR complex stability by forging stable interactions with an internal component of the complex, NADPH, and with the solvent, water. The oxygen atom in the DEAZ heterocyclic ring showed little net effect on the DEAZ heterocyclic ring interaction energy. Additionally, binding site and DHFR interactions were generally more favorable with the heterocyclic carbon atoms than with the nitrogen atoms.

The interaction energies of the carbon and oxygen atoms of the phenyl groups are shown in Figure 5 A-D. The oxygens are clearly important contributors to favorable phenyl interaction energies, especially in the cases of the binding site, DHFR, and complex interactions. These results indicate phenyl oxygen atoms generally participate in stabilizing the antifolate:complex interactions.

The interaction energies for the nitrogen, oxygen, and carbon atoms of the glutamyl regions are shown in Figure 6 A-D. With DEAZ, MTX, and MTX-$(glu)_3$, the oxygen atoms show stable binding site, DHFR, and complex interactions, while the carbon atoms show unstable interactions with these components. However, the nitrogen atoms showed very little net contribution to the glutamyl interaction energy. In the case of MTXT, both the oxygen and nitrogen atoms show stable interactions with the binding site, DHFR, and complex.

Figure 7 shows the conformation of the bound antifolate and its surrounding binding site residues for each DHFR complex. It should be noted that each antifolate imposes a somewhat different conformation on its binding site residues which likely contributes to differences in antifolate interaction energies.

DISCUSSION

An important objective of these studies was to evaluate interaction energies of DEAZ, MTX, MTX-$(glu)_3$, and MTXT with the solvated NADPH:human DHFR complex and its components, and to evaluate the contribution of the antifolate substructural regions to overall antifolate interaction energies.

The data in Figure 1 show that the interaction energy for each antifolate is derived primarily from its interaction with the binding site

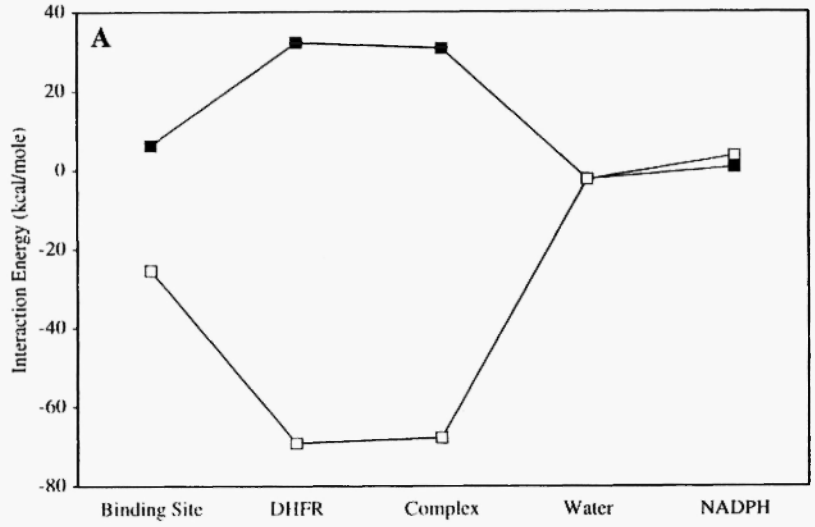

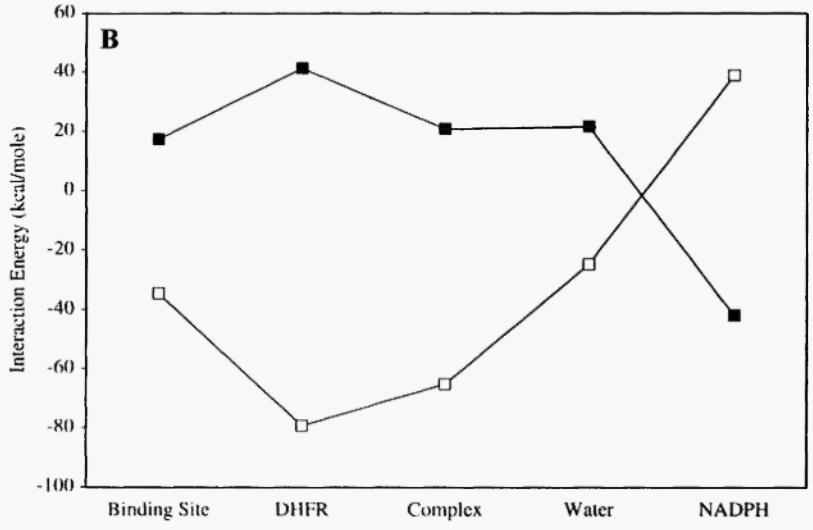

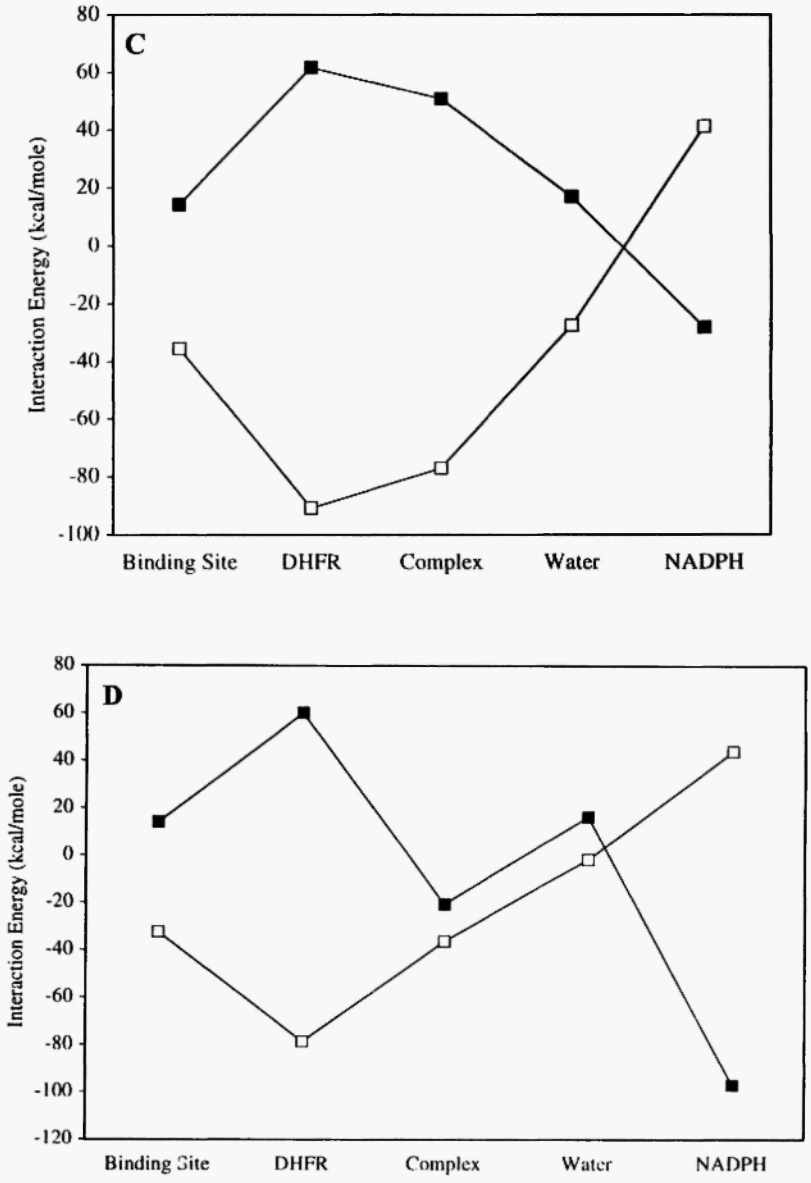

Fig. 5: Interaction energy analysis for the atomic subgroups of the phenyl moieties of 5,10-deazaaminopterin (panel A), MTX (panel B), MTX-$(glu)_3$ (panel C), and MTXT (panel D). The carbon and oxygen atoms atre represented by closed squares and open squares, respectively.

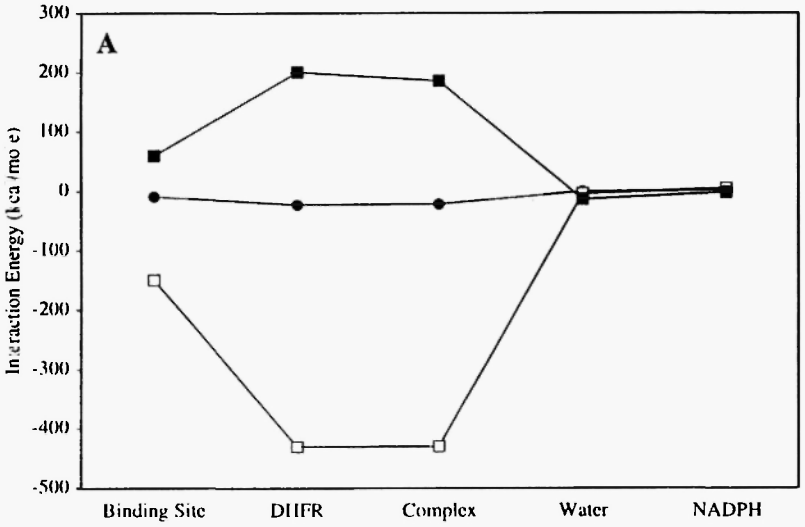

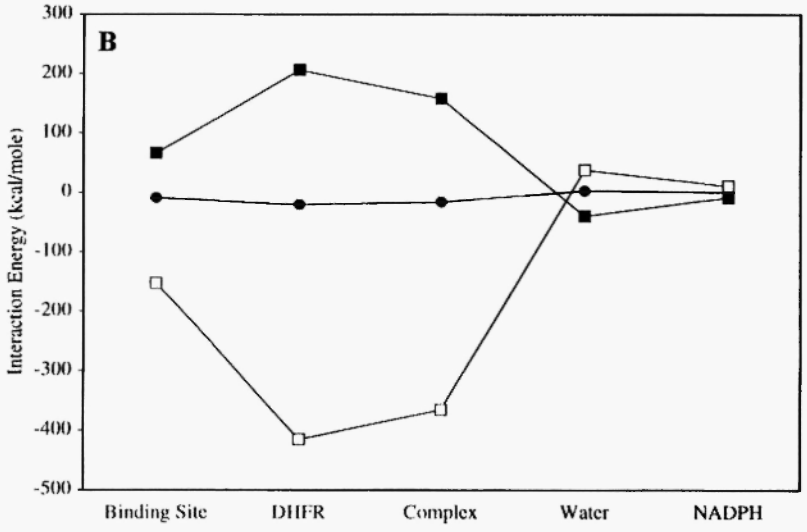

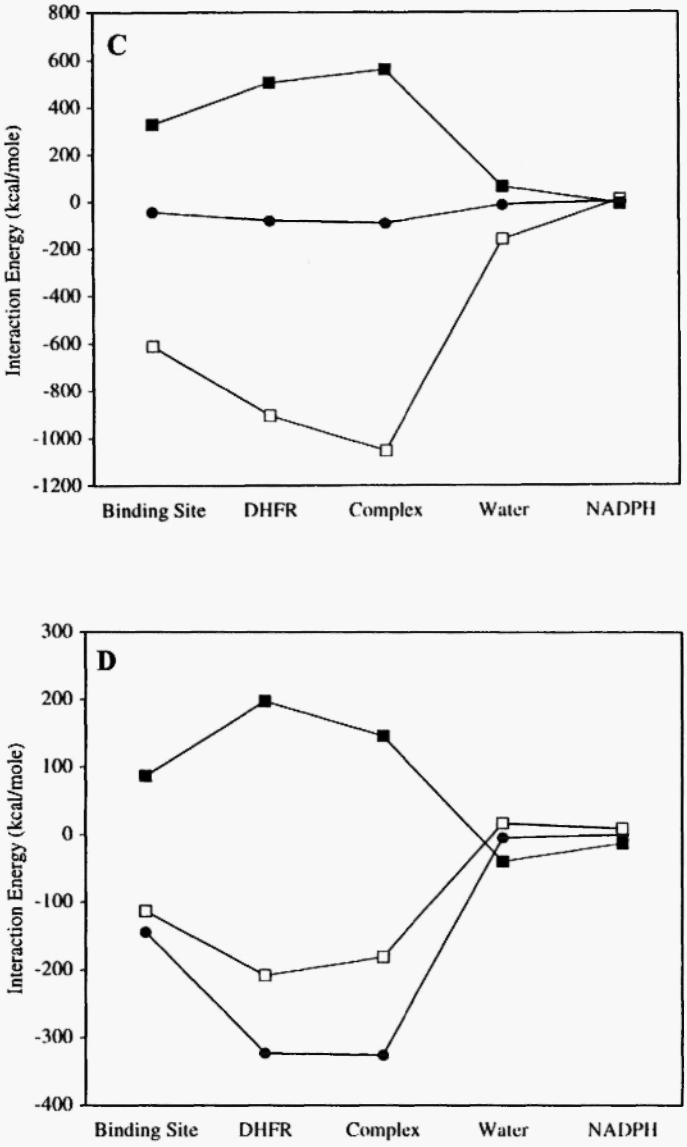

Fig. 6: Interaction energy analysis for the atomic subgroups of the glutamyl moieties of 5,10-deazaaminopterin (panel A), MTX (panel B), MTX-$(glu)_3$ (panel C), and MTXT (panel D). The nitrogen, carbon, and oxygen atoms are represented by closed circles, closed squares, and open squares, respectively.

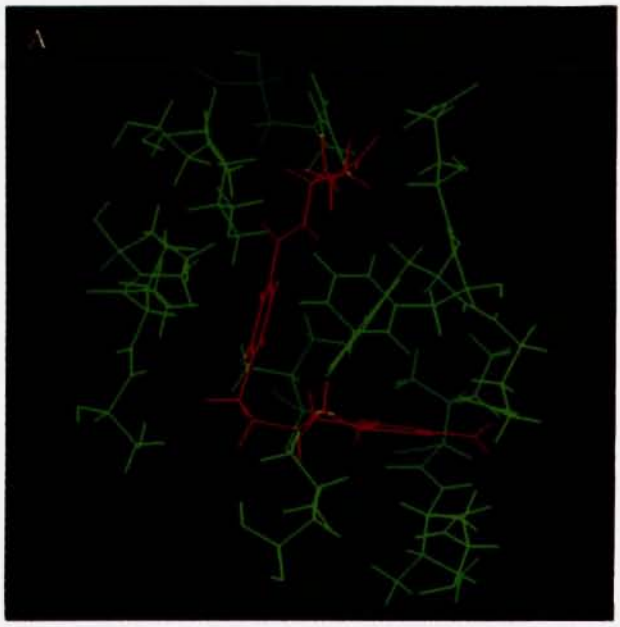

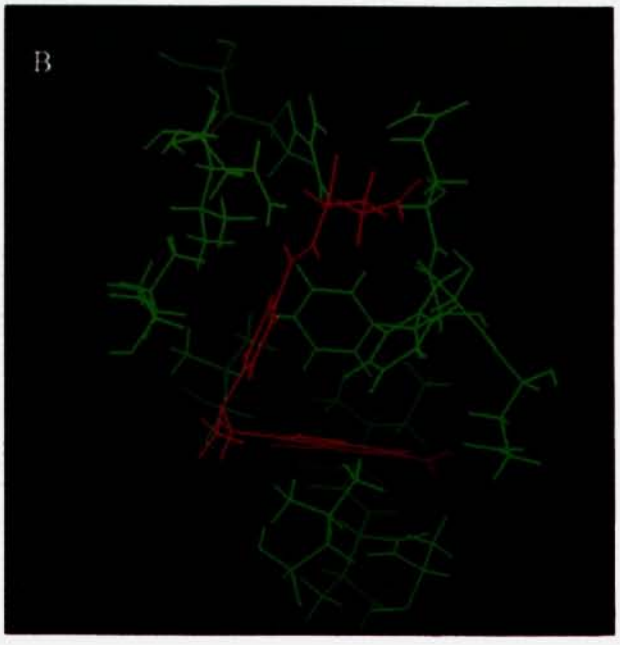

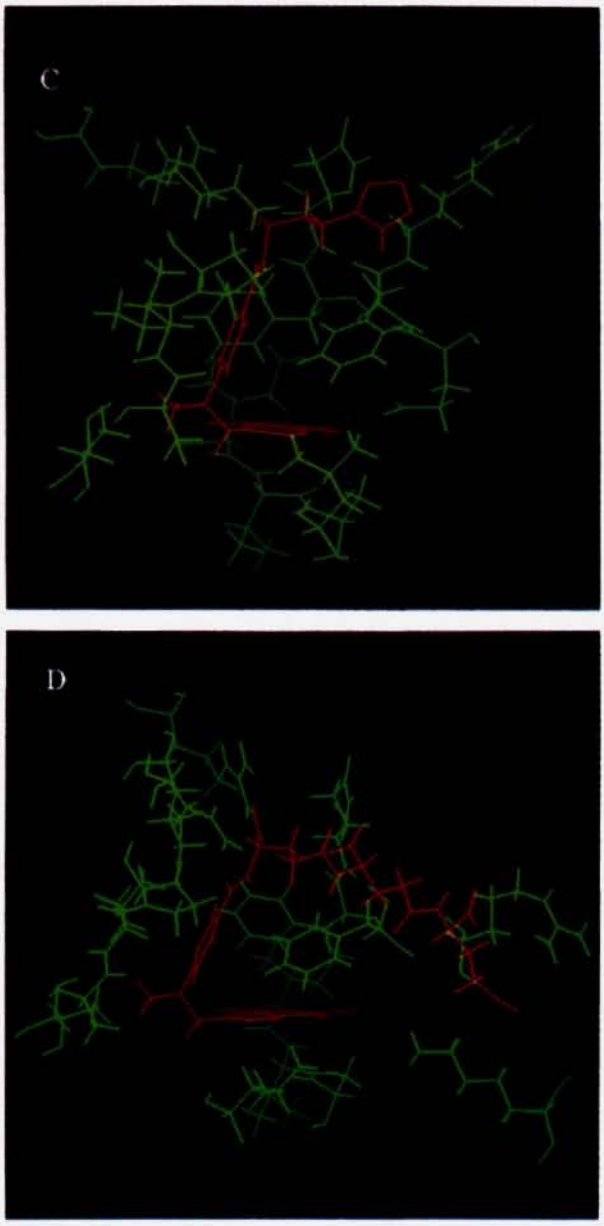

Fig. 7: Conformation of bound antifolates and their binding site residues. Red corresponds to bound antifolate; green corresponds to DHFR binding site residues. 5,10-Deazaaminopterin (Panel A), MTX (Panel B), MTXT (Panel C), and MTX-$(glu)_3$ (Panel D).

and DHFR. Antifolate interaction with water and NADPH showed much smaller contributions to stable interaction energies. From Figures 1 and 3, it can be seen that the glutamyl region is the primary stabilizing factor in the antifolate interactions. However, most of the glutamyl effect occurs with DHFR (Table 2). DHFR X-ray structures show that the glutamyl regions of bound antifolates are located on or near the protein surface /12/. Consequently, it was expected that the polar atoms of the glutamyl groups would display very stable interaction energies with water. However, much more favorable glutamyl interaction energies were observed with DHFR than with water. These observations suggest that the glutamyl groups participate more in DHFR interactions (presumably with surface residues) than with water.

Data presented in Figure 4 indicate that the interaction energies for the heterocyclic nitrogen atoms are generally unfavorable while the heterocyclic carbon atoms showed interactions that were generally favorable. Therefore, structural modifications of the heterocyclic moiety which result in an increase in the carbon atom/nitrogen atom ratio (C/N ratio) should result in more favorable interactions for the heterocyclic ring system. Rosowsky *et al.* /10/ synthesized 8-deaza, 5,8-deaza, and 5-methyl-5,8-deaza analogs of the DHFR inhibitor N^{alpha}-(4-amino-4-deoxypteroyl)-N^{delta}-hemiphthaloyl-L-ornithine. This compound has a heterocyclic ring system identical to that of MTX and aminopterin. Therefore, the deaza derivatives contained heterocyclic ring systems with an increased C/N ratio. As indicated earlier /10/ these deaza derivatives showed significant decreases in their Ki values for DHFR inhibition (i.e. 1.8, 3.8, and 3.5-fold lower, respectively, than for the unmodified compound). These observations clearly indicate that increasing the C/N ratio resulted in enhanced inhibitory effects of the analogs. These observations are consistent with the data presented in Figure 4. While the Ki values for the 5-deaza derivative appeared to be decreased relative to the parent compound, the magnitude of the decrease could not be considered statistically significant. Similar observations were made for the 5-deaza derivatives of aminopterin and MTX, which suggests that while increasing the C/N ratio of the heterocyclic system generally leads to improved binding, the magnitude of the difference observed is determined by the ring location of the deaza function /11,12/. Consequently, variation of the C/N ratio appears important in modulating

the interaction energy of the heterocyclic group and in the binding of the antifolate.

The glutamyl oxygen atoms are important in stabilizing the glutamyl interactions (Fig. 6). In each antifolate, the glutamyl oxygen atoms show the most stable interaction energies with the binding site, DHFR, and complex. The glutamyl nitrogen atoms of DEAZ, MTX-$(glu)_3$, and MTX showed interaction energies close to zero, while the nitrogen atoms of MTXT showed more stable interactions, which is likely due to the strong polarity of the tetrazole nitrogen atoms. Since glutamyl oxygens generally exhibit more favorable interactions than the glutamyl nitrogens, replacement of a glutamyl oxygen with nitrogen should result in decreased antifolate activity. Rosowsky *et al.* /4/ prepared gamma-monoamides of MTX and aminopterin. The resulting analogs contained fewer glutamyl oxygens and more glutamyl nitrogens. They exchanged an atom with a favorable interaction energy for an atom with a less favorable interaction energy. These investigators observed that the resulting analogs exhibited IC_{50} values against DHFR that were from 1.5 to 5-fold higher than those observed for parent compounds, which is also consistent with the data presented in Figure 6.

n-Octyl, n-dodecyl, and n-hexadecyl alpha and gamma esters of MTX were prepared by Rosowsky *et al.* /5/. These derivatives were all shown to be less effective than MTX as DHFR inhibitors. Additionally, the inhibitory effect continued to decrease as the number of carbon atoms in the esters was increased. These observations are consistent with the data in Figure 6, which indicate that the interactions of the glutamyl carbon atoms are generally unfavorable. Therefore, increasing the number of the carbon atoms in the glutamyl group enhances an unfavorable aspect of the interaction which should decrease the binding effectiveness of the analogs, as was observed /5/.

The above mentioned observations /4,5,10/ along with the data presented clearly suggest that interaction energy analyses may provide a very interesting and potentially useful method of identifying or targeting structural subregions within compounds for the continued development of new and improved therapeutic compounds.

CONCLUSION

These results clearly indicate that the different antifolate substructural regions make significantly different contributions to the overall antifolate interaction energy. As a result of identifying the contributions of antifolate substructural regions to antifolate binding stability, design strategies may be developed to specifically enhance the contribution of a particular substructural region to overall antifolate binding stability, resulting in more efficient DHFR inhibition.

ACKNOWLEDGEMENTS

This work was supported in part by grants RCMI-NIH 5G12RR 03048-13 and NIGMS-NIH S06GM0801628.

REFERENCES

1. Huennekens FM. The methotrexate story: a paradigm for development of cancer chemotherapeutic agents. Adv Enzyme Regul 1994; 34: 397-419.
2. Williams JW, Morrison JF, Duggleby RG. Methotrexate, a high-affinity pseudosubstrate of dihydrofolate reductase. Biochemistry 1979; 18: 2567-2573.
3. Rosowsky A, Forsch RA, Moran RG, Kohler W, Freisheim JH. Methotrexate analogues. 32. Chain extension, alpha-carboxyl deletion, and gamma-carboxyl replacement by sulfonate and phosphonate: effect on enzyme and cell-growth inhibition. J Med Chem 1988; 31: 1326-1331.
4. Rosowsky A, Bader H, Radike-Smith M, Cucchi CA, Wick MM, Freisheim JH. Methotrexate analogues. 28. Synthesis and biological evaluation of new gamma-monoamides of aminopterin and methotrexate. J Med Chem 1986; 29: 1703-1709.
5. Rosowsky A, Forsch RA, Yu CS, Lazarus H, Beardsley GP. Methotrexate analogues. 21. Divergent influence of alkyl chain length on the dihydrofolate reductase affinity and cytotoxicity of methotrexate monoesters. J Med Chem 1984; 27: 605-609.
6. McGuire JJ, Russell CA, Bolanowska WE, Freitag CM, Jones CS, Kalman TI. Biochemical and growth inhibition studies of methotrexate and aminopterin analogues containing a tetrazole ring in place of the gamma-carboxyl group. Cancer Res 1990; 50: 1726-1731.
7. Whitehead VM. Synthesis of methotrexate polyglutamates in L1210 murine leukemia cells. Cancer Res 1977; 37: 408-412.
8. Galivan J. Transport and metabolism of methotrexate in normal and resistant cultured rat hepatoma cells. Cancer Res 1979; 39: 735-743.

9. Kumar P, Kisliuk RL, Gaumont Y, Nair MG, Baugh CM, Kaufman BT. Interaction of polyglutamyl derivatives of methotrexate, 10-deazaaminopterin, and dihydrofolate with dihydrofolate reductase. Cancer Res 1986; 46: 5020-5023.
10. Rosowsky A, Wright JE, Vaidya CM, et al. Synthesis and potent antifolate activity and cytotoxicity of B-ring deaza analogues of the nonpolyglutamatable dihydrofolate reductase inhibitor N-alpha-(4-amino-4-deoxypteroyl)-N-delta-hemiphthaloyl-L-ornithine. J Med Chem 1998; 41: 5310-5319.
11. DeGraw JL, Christie PH, Kisliuk RL, Gaumont Y, Sirotnak FM. Synthesis and antifolate properties of 9-alkyl-10-deazaminopterins. J Med Chem 1990; 33: 212-215.
12. Sirotnak FM, Schimid FA, Otter GM, Piper JR, Montgomery JA. Structural design, biochemical properties, and evidence for improved therapeutic activity of 5-alkyl derivatives of 5-deazaaminopterin and 5-deazamethotrexate compared to methotrexate in murine tumor models. Cancer Res 1988; 48: 5686-5691.
13. Piper JR, Ramamurthy B, Johnson CA, Otter GM, Sirotnak FM. Analogues of 10-deazaaminopterin and 5-alkyl-5-10-dideazaaminopterin with the 4-substituted 1-naphthoyl group in the place of 4-substituted benzoyl. J Med Chem 1996; 39: 614-618.
14. Cody V, Luft JR, Ciszak E, Kalman TI, Freishein JH. Crystal structure determination at 2.3 Å of recombinant human dihydrofolate reductase ternary complex with NADPH and methotrexate-gamma-tetrazole. Anti-Cancer Drug Design 1992; 7: 483-491.
15. Brooks BR, Bruccoleri RE, Olafson BD, States DJ, Swaminathan S, Karplus M. CHARMM: a program for macromolecular energy, minimization, and dynamics caluclations. J Comput Chem 1983; 4: 187-217.